

Reconfigurable robotic machining system controlled and programmed in a machine tool manner

Dragan Milutinovic · Milos Glavonjic ·
Nikola Slavkovic · Zoran Dimic · Sasa Zivanovic ·
Branko Kokotovic · Ljubodrag Tanovic

Received: 11 March 2010 / Accepted: 5 August 2010 / Published online: 10 September 2010
© Springer-Verlag London Limited 2010

Abstract Industrial robots represent a promising cost-effective and flexible alternative for some machining applications. This paper describes the concept of reconfigurable robot multi-axis machining systems for machining the complex parts of light materials with lower tolerances having freeform surfaces. For the basic configuration of a five-axis robotic machining system, the robot modeling approach is shown in detail as well as the prototype of developed control system with programming in G-code. The experimental robotic machining system has been verified by successful machining of several test work pieces.

Keywords Robotic machining · Robot modeling · Control and programming system

1 Introduction

Over the last four decades, industrial robots were used to realize many industrial tasks like material handling, welding, assembly, spray painting, and auxiliary machining tasks, such as de-burring, polishing, grinding, etc. However, only 3% to 4% of the overall number of industrial robots is used for machining [1, 2]. Compared to machine tools, industrial

robots are cheaper and more flexible with potentially larger work space.

This is why researchers, robot, and CAD/CAM software manufactures as well as people from machining shops are enthusiastic to replace machine tools by robots for certain multi-axis milling applications. These include milling materials, such as clay, foam, wax, etc. for new product design, styling, and rapid prototyping projects [3–8]. Machining of work pieces of traditional materials, such as wood, stone, aluminum, etc. in which dimensional tolerances are low or even middle also produce satisfactory results [1, 9, 10].

It is widely recognized that poor accuracy, stiffness, and complexity of programming are the most important limiting factors for wider adoption of robotic machining in machine shops. Quite a lot of research in the field of robotic machining has been done to analyze the robot structure and to increase accuracy. The major fields of interest for robotic machining can be subdivided into kinematic, calibration, control, programming, and process development [2, 4, 9, 11, 12]. Also, the leading world robot manufactures are developing robotic arms specifically designed for robotic machining application [13]. The reason for the complexity of robot programming in machining application is in that each robot manufacturer uses, for the most part, its own proprietary robot programming language, because no industry standard exists. This fact was a strong motivation for both researchers and leading world robot and CAD/CAM software manufactures to develop versatile software solutions, such as G-code translators, specific postprocessor solutions, etc. to make the robot programming close to the programming efficiency of CNC machine tools [12, 13].

In order to contribute to efficient use of robots for machining applications, the reconfigurable robotic machining system controlled and programmed in machine tool

D. Milutinovic · M. Glavonjic (✉) · N. Slavkovic ·
S. Zivanovic · B. Kokotovic · L. Tanovic
Mechanical Engineering Faculty, University of Belgrade,
Kraljice Marije 16,
11120 Belgrade, Serbia
e-mail: mglavonjic@mas.bg.ac.rs

Z. Dimic
Lola Institute,
Belgrade, Serbia

manner is proposed [14]. This paper describes the concept of reconfigurable robot multi-axis machining systems for machining the complex parts of light materials with lower tolerances, having freeform surfaces. For the basic configuration of a five-axis robotic machining system, the robot modeling approach is shown in detail as well as the prototype of developed control system with programming in G-code. Finally, several test work pieces were machined to demonstrate the effectiveness of experimental robotic machining system.

2 The concept of reconfigurable robot based multi-axis machining system

The planned reconfigurable robot-based multi-axis machining system should provide rapid machining of larger-sized complex parts of light materials, with lower tolerances and with freeform surfaces generated by available CAD/CAM systems and reverse engineering methods.

The concept underlying the reconfigurable robot-based multi-axis machining system [14] (Fig. 1), presented briefly in this paper, is based on:

- The development of a specialized five-axis vertical articulated robot (Fig. 1a): larger workspace, higher payload, and stiffness, with integrated motor spindle, similar to [9] (<http://www.staubli.com/en/robotics/robot-solution-application/high-speed-machining-robot/>). Due to its advantages in respect of stiffness [1] and singularities [16], such a robot would operate as a vertical five-axis milling machine (X, Y, Z, A, B) spindle-tilting type [15].
- The possibilities of reconfiguring the system by applying the modular system of additional rotation and translation axes (Fig. 1b and c).
- Open architecture control based, at this stage, on PC real-time Linux platform and Enhanced Machine Control (EMC2) software system (<http://www.isd.mel.nist.gov/projects/rcslib/>, <http://www.linuxcnc.org/>).
- The possibilities of programming a robot as a vertical five-axis milling machine in G-code.
- The possibilities of using the existing CAD/CAM systems with implemented three- to five-axis machining for vertical milling machines (X, Y, Z, A, B) spindle-tilting type.
- Virtual robotic machining system configured in object-oriented programming language Python implemented in the control system for program simulation and verification.

As noticeable, the basic goal of the planned system, partially presented in this paper, is to be directly applicable in machine shops by personnel experienced in CNC

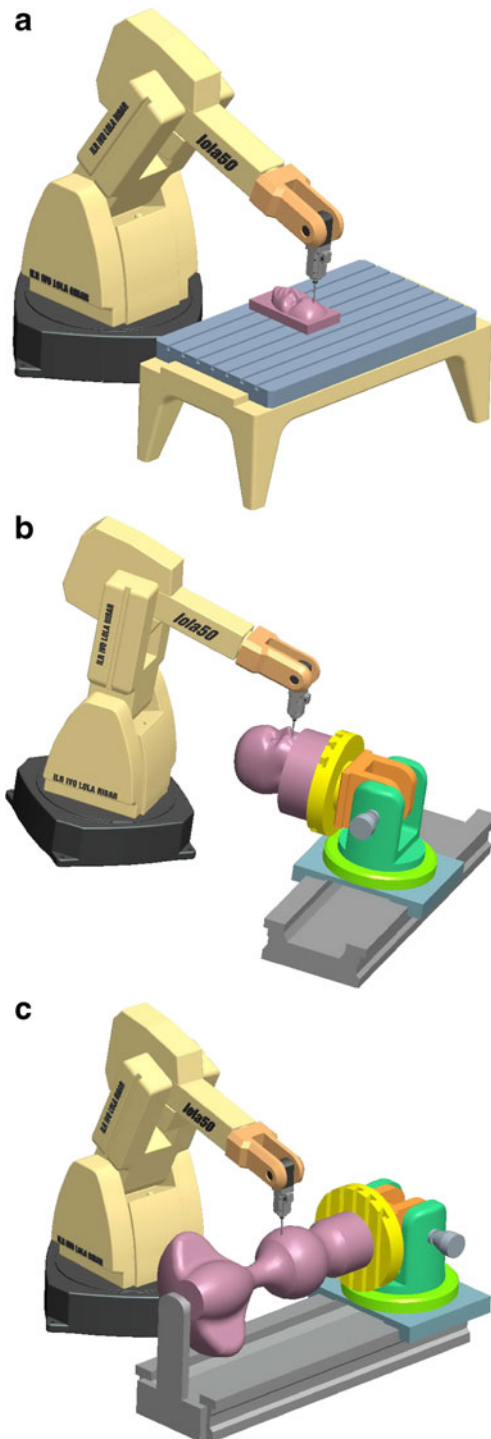


Fig. 1 a–c Conceptual model of reconfigurable robot-based multi-axis machining system

technology and programming in G-code that is still very widespread in industry [17].

To verify the concept and for the development of control and programming system, a standardized six-axis vertical articulated robot (with payload of 50 kg; Fig. 2) was used as a testbed, in the way that the axis number 6 was blocked.

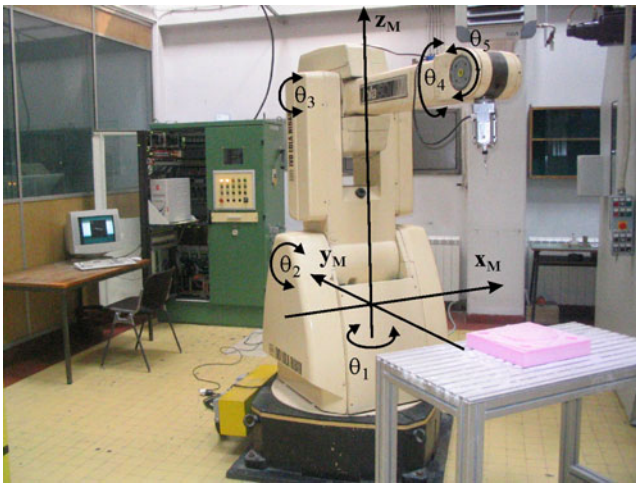


Fig. 2 The experimental five-axis robotic machining system in reference position

The robot is equipped with a high speed motor spindle with maximum speed of 18,000 rpm.

As evident from Fig. 2, the experimental five-axis robotic machining system is further considered as a five-axis vertical milling machine (X, Y, Z, A, B) spindle-tilting type, where machining is performed on a work table in front of the robot. The configured system as well as limited motions in joints relative to the reference position provide for:

- conveniences related to stiffness,
- taking into account only one solution of inverse kinematics,
- avoiding the robot singularities.

The problems of stiffness analyses, calibration, and compensation, even though of critical importance, as it is well-known [9, 11, 16], are not considered in this paper.

3 Kinematic modeling

The five-axis vertical articulated robot for complex surfaces machining (Figs. 1a, 2) will be considered in this paper as a specific configuration of the five-axis vertical milling machine (X, Y, Z, A, B) spindle-tilting type.

To adequately control the position and orientation of the tool during machining processes, kinematic model is required to establish mathematics description for the robot. In this paper, kinematic modeling involves solving of direct and inverse kinematics and a brief analysis of the robot workspace for the cases of three-axis and five-axis machining.

3.1 Joint and world coordinates

Figure 3 represents a geometric model of the robot. The robot reference frame {M} has been adopted according to

the standard for this machine type [18]. The tool frame {T} is attached to the milling tool at the tool tip T, so that the axis z_T coincides with tool axis and the frame {W} is attached to the work piece. Vectors v referenced in frames {M} and {W} are denoted by $^M v$ and $^W v$.

To solve direct and inverse kinematics, joint and world coordinates will be defined first.

3.1.1 Joint coordinates vector

For this five-axis vertical articulated robot, joint coordinate vector is represented as

$$\theta = [\theta_1 \ \theta_2 \ \theta_3 \ \theta_4 \ \theta_5]^T \tag{1}$$

where $\theta_i, i = 1, 2, \dots, 5$ are scalar joint variables controlled by actuators.

3.1.2 World coordinates

As it is known, the CAD/CAM system calculates a tool path defined by a set of successive tool positions and orientations expressed in the work piece frame {W} (Fig. 3). The calculated tool path is machine independent and is known as a cutter location file (CL file). A tool position is given by the position vector of the tool tip T in the work piece frame {W} as

$$^W p_T = [x_t \ y_t \ z_t]^T \tag{2}$$

and the tool orientation is given by unit vector associated to the tool axis direction as

$$^W k_T = [k_{tx} \ k_{ty} \ k_{tz}]^T \tag{3}$$

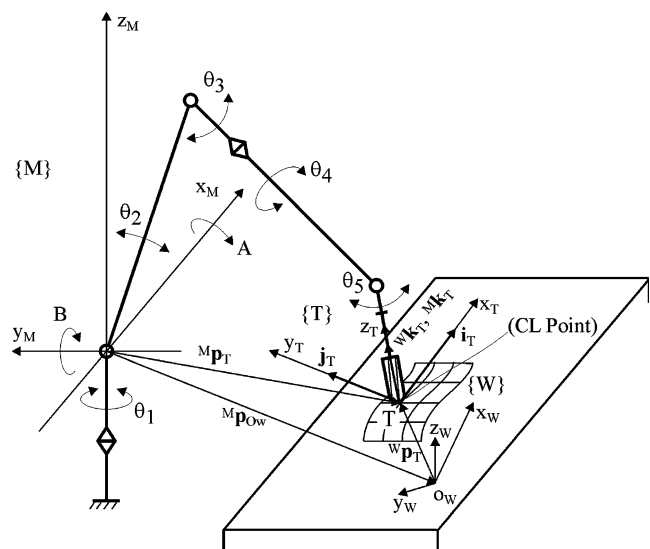


Fig. 3 Tool position and orientation in the work piece frame {W} and robot reference frame {M}

As the axes of frames {M} and {W} need not be parallel, the tool tip position vector and unit vector of tool axis direction in the robot reference frame {M} can be expressed as

$${}^M\mathbf{p}_T = [x_M \ y_M \ z_M]^T = {}^M\mathbf{p}_{Ow} + {}^M_W R \cdot {}^W\mathbf{p}_T \tag{4}$$

$${}^M\mathbf{k}_T = [k_{Tx} \ k_{Ty} \ k_{Tz}]^T = {}^M_W R \cdot {}^W\mathbf{k}_T \tag{5}$$

where ${}^M\mathbf{p}_{Ow} = [x_{Ow} \ y_{Ow} \ z_{Ow}]^T$ is the position vector of the origin of work piece frame {W}. It should be noted that determining of the position vector ${}^M\mathbf{p}_{Ow}$ and orientation of the work piece frame {W} is conducted according to the procedure for five-axis CNC machine tools and thereafter the orientation matrix ${}^M_W R$ in Eqs. 4 and 5 is determined and executed in control system.

In order to make a set of world coordinates complete, it is also needed to determine the tool orientation angles A and B which define only the direction of tool axis z_T . As can be seen from Fig. 3, the tool axis z_T also coincides with the axis of the last link of the robot for which motor spindle is attached. Since robot has 5 DOF, only the direction of the z_T axis is controllable, while the axes x_T and y_T will have uncontrollable rotation about the axis z_T .

The description of the position and orientation of one frame relative to another e.g. in this case of the frame {T} relative to the frame {M} can be represented through homogenous coordinate transformation matrix 4×4 , [19–21], as

$${}^M_T T = \begin{bmatrix} {}^M_T R & {}^M\mathbf{p}_T \\ 0 & 0 & 0 & 1 \end{bmatrix} = \begin{bmatrix} i_{Tx} & j_{Tx} & k_{Tx} & x_M \\ i_{Ty} & j_{Ty} & k_{Ty} & y_M \\ i_{Tz} & j_{Tz} & k_{Tz} & z_M \\ 0 & 0 & 0 & 1 \end{bmatrix} \tag{6}$$

where rotation matrix ${}^M_T R$ represents the orientation, while vector ${}^M\mathbf{p}_T$ represents the position of the frame {T} with respect to the robot reference frame {M}. To bring the tool axis, i.e., the axis z_T of the frame {T} to a desirable angular position with respect to the frame {M}, the frame {T} must be rotated first about the axis x_M by the angle A , and then about the axis y_M by the angle B , as prescribed by the convention for five-axis machine tools (X, Y, Z, A, B) spindle-tilting type. The derivation of equivalent rotation matrix ${}^M_T R$ can be further derived as

$${}^M_T R = R_{yM,B} \cdot R_{xM,A} = \begin{bmatrix} cB & sA \cdot sB & cA \cdot sB \\ 0 & cA & -sA \\ -sB & sA \cdot cB & cA \cdot cB \end{bmatrix} = \begin{bmatrix} i_{Tx} & j_{Tx} & k_{Tx} \\ i_{Ty} & j_{Ty} & k_{Ty} \\ i_{Tz} & j_{Tz} & k_{Tz} \end{bmatrix} \tag{7}$$

where rotation matrices

$$R_{xM,A} = \begin{bmatrix} 1 & 0 & 0 \\ 0 & cA & -sA \\ 0 & sA & cA \end{bmatrix} \text{ and } R_{yM,B} = \begin{bmatrix} cB & 0 & sB \\ 0 & 1 & 0 \\ -sB & 0 & cB \end{bmatrix} \tag{8}$$

are so-called basic rotation matrices [20]. “c” and “s” refer to cosine and sine functions.

Given that it is of interest only the direction of the tool axis z_T specified by unit vector ${}^M\mathbf{k}_T = [k_{Tx} \ k_{Ty} \ k_{Tz}]^T$ whose description is above given, by equating the corresponding members of matrix ${}^M_T R$ from Eq. 7 the angles A and B can be determined as

$$A = A \tan 2(-k_{Ty}, \sqrt{1 - k_{Ty}^2}) \tag{9}$$

and

$$B = A \tan 2\left(\frac{k_{Tx}}{cA}, \frac{k_{Tz}}{cA}\right) \tag{10}$$

Although in Eq. 9, a second solution exists, by using the positive square root the single solution for which $-90^\circ \leq A \leq 90^\circ$ is always computed [15, 21]. This way, the world coordinates vector can be expressed as

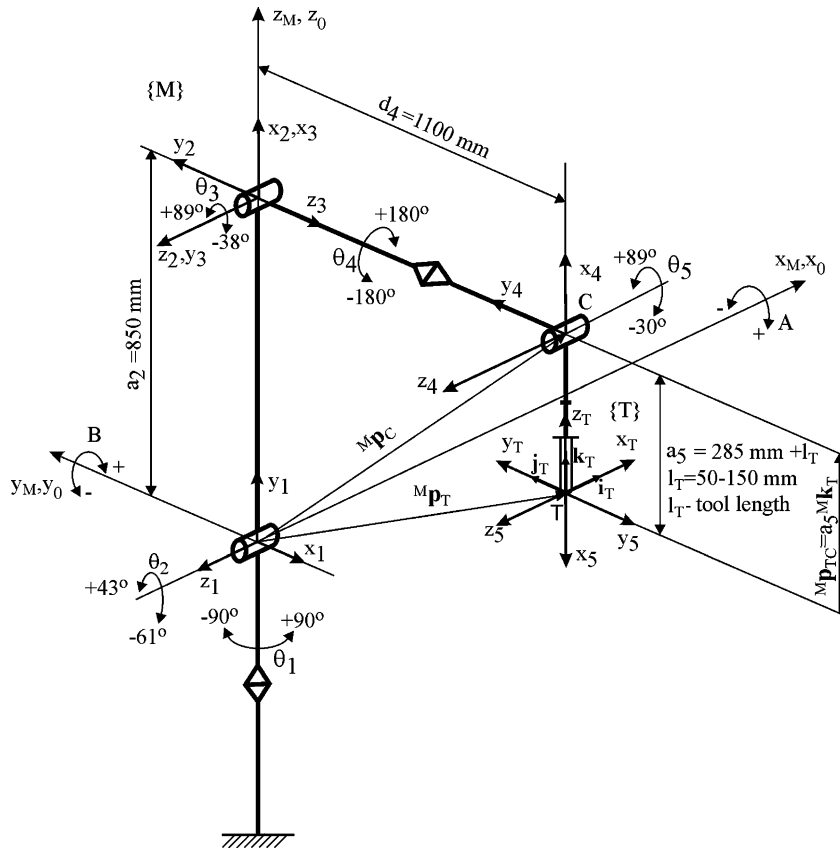
$$\mathbf{x} = [x_M \ y_M \ z_M \ A \ B]^T \tag{11}$$

3.2 Direct and inverse kinematics

To model the robot, the Denavit–Hartenberg (D–H) notation [19–21] was used in this research owing to its simplicity and popularity in the robotics community. As noticeable from Fig. 3, the robot has five moving links connected together by five rotational joints. The first moving link is connected with the supporting base, while the last link is attached with a tool. To perform kinematic analysis, first, coordinate frames are rigidly attached to each link. Relative position and orientation between these coordinate frames can be described using homogeneous transformations. The homogeneous transformation describing the relation between one link and the next link is traditionally referred to as an A matrix. Matrix ${}^i_{i-1}A$ designates D–H transformation matrix relating frame (i) to frame ($i-1$). Figure 4 shows D–H coordinate frames for the experimental five-axis robot from Figs. 2 and 3 in the reference position.

The D–H model adopts four parameters ($a_i, \alpha_i, d_i, \theta_i$) to describe the transformation, including translations and rotations from link ($i-1$) to link (i). The first parameter a_i represents the length of common normal of the two link axes. The second parameter α_i denotes the angle between the two link axes. The remaining two parameters describe relative position of two adjacent links, which are provided by their distance, d_i , and their rotation θ_i .

Fig. 4 Link coordinate frames for the experimental five-axis machining robot in the reference position



After the D–H coordinate frame is assigned to each link, the transformation between successive frames ($i-1$) and (i) is described as follows:

$${}^{i-1}A = Rot(z_{i-1}, \theta_i) \cdot Trans(0, 0, d_i) \cdot Trans(a_i, 0, 0) \cdot Rot(x_i, \alpha_i)$$

$$= \begin{bmatrix} c\theta_i & -c\alpha_i \cdot s\theta_i & s\alpha_i \cdot s\theta_i & a_i \cdot c\theta_i \\ s\theta_i & c\alpha_i \cdot c\theta_i & -s\alpha_i \cdot c\theta_i & a_i \cdot s\theta_i \\ 0 & s\alpha_i & c\alpha_i & d_i \\ 0 & 0 & 0 & 1 \end{bmatrix} \quad (12)$$

Prior to making the list of D–H parameters complete for each link of the robot, it is needed to make a few important remarks and specify constraints:

- The robot reference frame $\{M\}$ adopted according to the standard for five-axis vertical milling machine (X, Y, Z, A, B) spindle-tilting type coincides with the robot base frame (x_0, y_0, z_0) .
- To make the robot reference position correspond the reference position for adopted five-axis vertical milling machine (X,Y,Z,A,B) spindle-tilting type, first joint was rotated by $\theta_1 = -90^\circ$, second joint by $\theta_2 = 90^\circ$, fifth joint by $\theta_5 = 180^\circ$ and the tool frame $\{T\}$ was introduced according to Fig. 3.

- The ranges of joints motions are specified relative to thus adopted robot reference position and are lower compared to the experimental robot’s real capacities. The adopted ranges of joints motions, Fig. 4, enable only the choice of those solutions of inverse kinematics, which are logical for machining and avoid singularities.
- For the joint angle θ_4 the convention has been changed to facilitate the operator’s work related with the tool orientation angle B.

Considering the above mentioned remarks and constraints a list of D–H kinematic parameters for each link is shown in Table 1.

Substituting D–H parameters of the links from Table 1 in Eq. 12 the transformation matrices ${}^{i-1}A, i = 1, 2, \dots, 5$ are obtained.

Table 1 D–H kinematic parameters

Link i	$\alpha_i [^\circ]$	$a_i [mm]$	$d_i [mm]$	$\theta_i [^\circ]$
1	90	0	0	$\theta_1 - 90$
2	0	a_2	0	$\theta_2 + 90$
3	90	0	0	θ_3
4	-90	0	d_4	$-\theta_4$
5	0	a_5	0	$\theta_5 + 180$

As mentioned above, considering that the robot is observed in the present paper as a five-axis vertical milling machine (X, Y, Z, A, B) spindle-tilting type, the importance is given to the frame {T} whose axis z_T must coincide with the tool axis. As noticeable from Fig. 4, the frame {T} can be described relative to the frame (x_5, y_5, z_5) by homogeneous transformation matrix as

$${}^5_7T = \begin{bmatrix} 0 & 0 & -1 & 0 \\ 0 & -1 & 0 & 0 \\ -1 & 0 & 0 & 0 \\ \hline 0 & 0 & 0 & 1 \end{bmatrix} \quad (13)$$

3.2.1 Direct kinematics

Now, as it is well known [19–21], the tool position and orientation, i.e., the position and orientation of frame {T} with respect to the robot reference frame {M} (Fig. 4) for the given joint coordinates vector θ and specified link parameters can be determined as

$${}^M_7T = {}^0_1A \cdot {}^1_2A \cdot {}^2_3A \cdot {}^3_4A \cdot {}^4_5A \cdot {}^5_7T = \begin{bmatrix} {}^M_7R & {}^M\mathbf{p}_T \\ \hline 0 & 0 & 0 & 1 \end{bmatrix} = \begin{bmatrix} i_{Tx} & j_{Tx} & k_{Tx} & x_M \\ i_{Ty} & j_{Ty} & k_{Ty} & y_M \\ i_{Tz} & j_{Tz} & k_{Tz} & z_M \\ \hline 0 & 0 & 0 & 1 \end{bmatrix} \quad (14)$$

where further consideration are of significance only

$$\begin{aligned} k_{Tx} &= -s\theta_1 \cdot s\theta_{23} \cdot c\theta_4 \cdot c\theta_5 + c\theta_1 \cdot s\theta_4 \cdot c\theta_5 - s\theta_1 \cdot c\theta_{23} \cdot s\theta_5 \\ k_{Ty} &= c\theta_1 \cdot s\theta_{23} \cdot c\theta_4 \cdot c\theta_5 + s\theta_1 \cdot s\theta_4 \cdot c\theta_5 + c\theta_1 \cdot c\theta_{23} \cdot s\theta_5 \\ k_{Tz} &= c\theta_{23} \cdot c\theta_4 \cdot c\theta_5 - s\theta_{23} \cdot s\theta_5 \\ x_M &= -a_5 \cdot k_{Tx} + s\theta_1 \cdot (d_4 \cdot c\theta_{23} - a_2 \cdot s\theta_2) \\ y_M &= -a_5 \cdot k_{Ty} - c\theta_1 \cdot (d_4 \cdot c\theta_{23} - a_2 \cdot s\theta_2) \\ z_M &= -a_5 \cdot k_{Tz} + d_4 \cdot s\theta_{23} + a_2 \cdot c\theta_2 \end{aligned} \quad (15)$$

and where $\theta_{ij} = \theta_i + \theta_j$.

In Eq. 15, apart from the position of tool tip in the reference frame {M} ${}^M\mathbf{p}_T = [x_M \ y_M \ z_M]^T$, the third column of rotation matrix M_7R was also calculated. As the robot has 5 DOF, only the direction of the tool axis z_T is controllable, while the axes x_T and y_T will have uncontrollable rotation about the axis z_T . This means that through the vector ${}^M\mathbf{k}_T = [k_{Tx} \ k_{Ty} \ k_{Tz}]^T$ from the Eq. 15, the angles A and B can be determined using Eqs. 9 and 10. This way, the world coordinates vector has been completed, i.e., direct kinematics problem is solved.

3.2.2 Inverse kinematics

The method for closed-form solution of inverse kinematics of 6 DOF robots with the last three joint axes intersecting at a point or with three consecutive parallel joint axes is referred to as Pieper’s method. This method enables the decoupling of inverse kinematic problem in two simpler problems known as inverse position kinematics and inverse orientation kinematics. A detailed description of this method has been given in [21, 22]. A closed-form solution of general 5 DOF robots with revolute joints has been considered in several papers. In [23], the possibility is considered, in general, of finding the closed-form solution of inverse kinematics of five-revolute-axis robots with two intersecting joint axes by applying Pieper’s method. In [24], similar possibility is also reported.

As noticeable from Fig. 4, the last two joint axes z_3 and z_4 intersect at point C (wrist center). This fact and the above presented remarks and constraints make possible to consider this 5 DOF robot as a special case of 6 DOF robot with the last three joint axes intersecting at a point. The solution of inverse kinematics will be partially geometric and partially algebraic.

As it can be concluded from Fig. 4, the position of wrist center C is influenced only by joint coordinates θ_1, θ_2 , and θ_3 . For the specified position vector of tool tip ${}^M\mathbf{p}_T = [x_M \ y_M \ z_M]^T$ and specified tool orientation angles A and B the rotation matrix M_7R from Eq. 7 is calculated first. Then, by using only unit vector ${}^M\mathbf{k}_T$ from calculated rotation matrix M_7R , the position vector of the wrist point C can be calculated as

$${}^M\mathbf{p}_C = \begin{bmatrix} x_C \\ y_C \\ z_C \end{bmatrix} = {}^M\mathbf{p}_T + {}^M\mathbf{p}_{TC} = {}^M\mathbf{p}_T + a_5 \cdot {}^M\mathbf{k}_T = \begin{bmatrix} x_M + a_5 \cdot k_{Tx} \\ y_M + a_5 \cdot k_{Ty} \\ z_M + a_5 \cdot k_{Tz} \end{bmatrix} \quad (16)$$

Based on the calculated components of position vector ${}^M\mathbf{p}_C$ from Eq. 16, inverse position kinematics will be solved using the geometric approach. Considering again the above explanations related to the reference frame {M}, reference robot position, and constraints of the ranges of joints motions to avoid multiple solutions and arm singularities, the angles θ_1, θ_2 , and θ_3 are geometrically solved from Fig. 5.

Observing the projection of the wrist center C in plane $(x_M, -y_M)$ and considering the robot reference position it is measured relative to, the angle θ_1 can be calculated as

$$\theta_1 = A \tan 2(x_C, -y_C) \quad (17)$$

As θ_1 is in the range $(-90^\circ, 90^\circ)$, i.e., as it is always $y_C < 0$, it means that arguments in the $A \tan 2$ function unambiguously determine the value of the variable θ_1 .

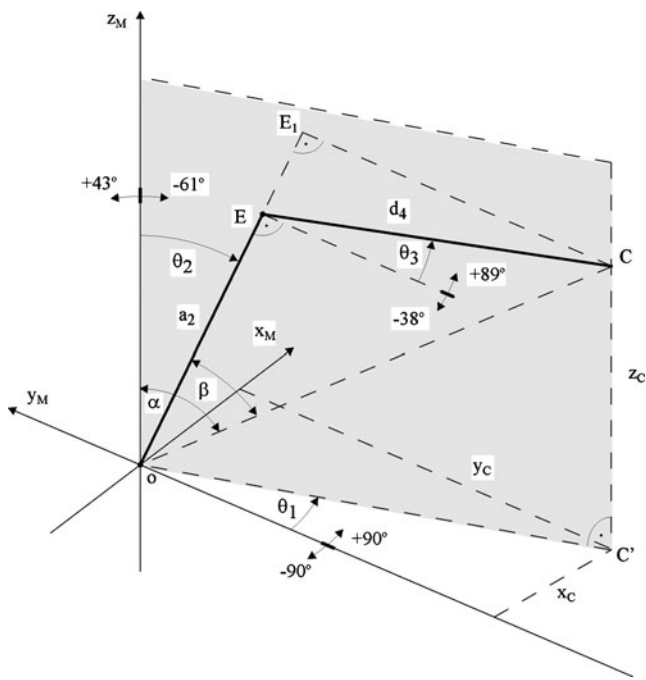


Fig. 5 Projection of the wrist center C onto $(x_M, -y_M)$ plane and onto shaded plane formed by links 2 and 3

Observing the projection of the wrist center C in the shaded plane formed by links 2 and 3, joint variables θ_2 and θ_3 can be calculated. From the triangle OCE, $s\theta_3$ can be determined through the law of cosines as

$$s\theta_3 = \frac{x_C^2 + y_C^2 + z_C^2 - a_2^2 - d_4^2}{2 \cdot a_2 \cdot d_4} \tag{18}$$

Considering that θ_3 is in the range of $(-38^\circ, 89^\circ)$, the only solution to be adopted is

$$\theta_3 = A \tan 2(s\theta_3, \sqrt{1 - s\theta_3^2}) \tag{19}$$

As it is known, the solution for the angle θ_3 influences the solution for the angle θ_2 . Using the adopted solution for θ_3 and for the angles α and β that can be determined from the triangles $OC'C$ and OCE_1 , the angle θ_2 can be determined as

$$\theta_2 = A \tan 2(-\sqrt{x_C^2 + y_C^2}, z_C) + A \tan 2(d_4 \cdot c\theta_3, a_2 + d_4 \cdot s\theta_3) \tag{20}$$

where it is taken into account the robot reference position that the angle θ_2 is measured relative to, which is within the range of $(-61^\circ, 43^\circ)$.

For the calculated values of joint coordinates θ_1 , θ_2 , and θ_3 , it is then shown the algebraic manner of solving inverse orientation kinematics, i.e., calculation of joint coordinates θ_4 and θ_5 .

It is started from the Eq. 14 written as

$${}^M T = {}^M T_3 \cdot {}^3 T = \begin{bmatrix} {}^M R & {}^M p_T \\ 0 & 1 \end{bmatrix} = \begin{bmatrix} * & * & {}^M k_T & {}^M p_T \\ 0 & 0 & 0 & 1 \end{bmatrix} \tag{21}$$

Substituting the matrices ${}^{i-1} A$, $i = 1, 2, 3$, Eq. 12, with previously solved joint variables θ_1, θ_2 , and θ_3 , it is obtained

$${}^M T = {}^0 A \cdot {}^1 A \cdot {}^2 A \cdot {}^3 A = \begin{bmatrix} {}^M R(\theta_1, \theta_2, \theta_3) & * \\ 0 & 0 & 0 & 1 \end{bmatrix} \tag{22}$$

Thereafter, substituting the matrices ${}^{i-1} A$, $i = 4, 5$, Eq. 12, with unknown joint variables θ_4 and θ_5 it is obtained

$${}^3 T = {}^3 A \cdot {}^4 A \cdot {}^5 T = \begin{bmatrix} * & * & {}^3 k_T(\theta_4, \theta_5) & * \\ 0 & 0 & 0 & 1 \end{bmatrix} \tag{23}$$

The elements of matrices in preceding equations denoted by asterisks are not shown because they are not of importance for these considerations. As it is possible to control only the tool orientation axis z_T , from Eqs. 21 to 23, it is obvious that

$${}^M k_T = {}^M R(\theta_1, \theta_2, \theta_3) \cdot {}^3 k_T(\theta_4, \theta_5) \tag{24}$$

From Eq. 24, the vector ${}^3 k_T$ can be determined now as

$${}^3 k_T = {}^M R^{-1} \cdot {}^M k_T \tag{25}$$

i.e., according to Eqs. 21 to 23 as

$$\begin{bmatrix} c\theta_4 \cdot c\theta_5 \\ -s\theta_4 \cdot c\theta_5 \\ -s\theta_5 \end{bmatrix} = \begin{bmatrix} -s\theta_1 \cdot s\theta_{23} \cdot k_{Tx} + c\theta_1 \cdot s\theta_{23} \cdot k_{Ty} + c\theta_{23} \cdot k_{Tz} \\ -c\theta_1 \cdot k_{Tx} - s\theta_1 \cdot k_{Ty} \\ s\theta_1 \cdot c\theta_{23} \cdot k_{Tx} - c\theta_1 \cdot c\theta_{23} \cdot k_{Ty} + s\theta_{23} \cdot k_{Tz} \end{bmatrix} \tag{26}$$

Having in mind that $-30^\circ \leq \theta_5 \leq 89^\circ$, from Eq. 26, the joint angle θ_5 can be determined as

$$\theta_5 = A \tan 2(s\theta_5, c\theta_5) \tag{27}$$

where

$$s\theta_5 = -s\theta_1 \cdot c\theta_{23} \cdot k_{Tx} + c\theta_1 \cdot c\theta_{23} \cdot k_{Ty} - s\theta_{23} \cdot k_{Tz} \tag{28}$$

and

$$c\theta_5 = \sqrt{1 - s\theta_5^2} \tag{29}$$

From Eq. 26, it is also calculated the joint angle θ_4 as

$$\theta_4 = A \tan 2(s\theta_4, c\theta_4) \tag{30}$$

where

$$c\theta_4 = (-s\theta_1 \cdot s\theta_{23} \cdot k_{Tx} + c\theta_1 \cdot s\theta_{23} \cdot k_{Ty} + c\theta_{23} \cdot k_{Tz}) / c\theta_5 \tag{31}$$

and

$$s\theta_4 = (-c\theta_1 \cdot k_{Tx} - s\theta_1 \cdot k_{Ty}) / (-c\theta_5) \tag{32}$$

whereby the solution of inverse kinematics problem is completed.

3.3 Workspace analysis

Based on inverse kinematics, it is possible to determine the position and orientation workspace of the robot considered here as a vertical five-axis milling machine. The applied approach proved to be very useful despite being based on the definition of position and orientation workspace for parallel kinematic chains [25].

In the case of the robot considered in this paper, the position and orientation workspace

$$Ws(x_M, y_M, z_M, A, B) = \{0, 1\} \tag{33}$$

is a Boolean function whose value is equal to 1 if the tool pose-defined by the quintet (x_M, y_M, z_M, A, B) is reachable without exceeding the limited motion range of the joints. Starting from the selected point in workspace volume, the estimation is made by specific step-by-step strategy that

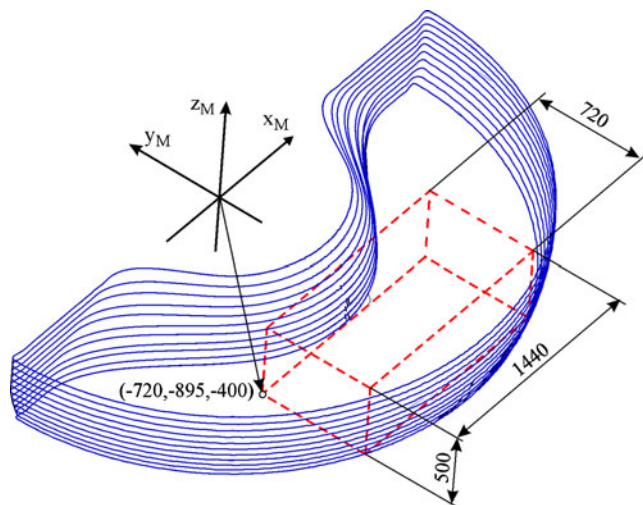


Fig. 6 Workspace in the case of three-axis machining ($A=0^\circ, B=0^\circ$)

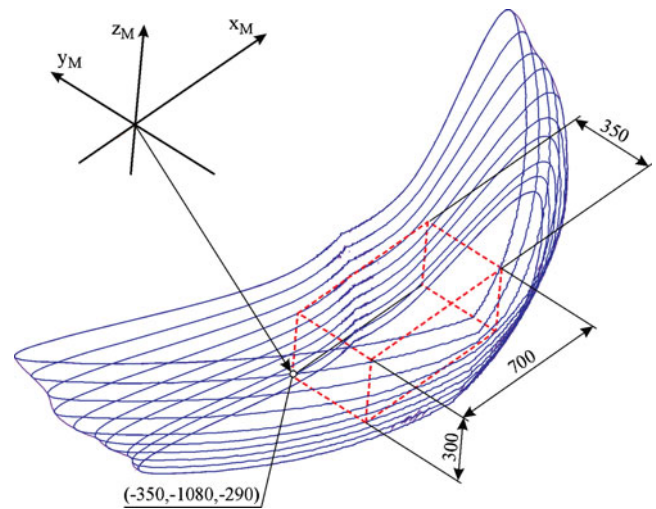


Fig. 7 Workspace in the case of five-axis machining with tool orientation angles in the ranges of $A [-30^\circ, 30^\circ]$ and $B [-30^\circ, 30^\circ]$

locates tool in one pose in the workspace and that determines whether the pose is reachable or not by taking into account a limited motion range of the joints given in Fig. 4.

The first step was to determine workspace for three-axis machining ($A = 0^\circ, B = 0^\circ$). A portion of workspace within boundaries logical for machining ($z_{min} = -400 \text{ mm}, z_{max} = 100 \text{ mm}$) is shown in Fig. 6. Thereafter, for the adopted ranges of tool orientation angles $A [-30^\circ, 30^\circ]$ and $B [-30^\circ, 30^\circ]$, workspace for five-axis machining was determined. A portion of workspace within boundaries logical for machining ($z_{min} = -350 \text{ mm}, z_{max} = 100 \text{ mm}$) is shown in Fig. 7. As it is well-known from practice, this workspace can be extended beyond this shape in the cases when intensive work should be done within narrower boundaries of orientation angles A and B .

For programmers and operators familiar with CNC machine tools, both of these workspaces can be reduced to the parallelepiped as indicated in Figs. 6 and 7.

4 Control and programming system

This section gives a brief description of the first prototype of the open architecture control (OAC) system for robotic machining system from Fig. 1a, implemented in the experimental five-axis vertical articulated machining robot, Fig. 2. One of the distinctive features of the concept of reconfigurable robot based multi-axis machining system, described in Section 2, is that it is applicable directly by CNC machine tool programmers by using the existing CAD/CAM systems and programming in G-code. Among several proposed OAC solutions, the development of the first low-cost control system prototype is based on PC real-

time Linux platform with EMC2 software for computer control of machine tools, robots, parallel kinematic machines [26], etc. EMC2 was initially created by the National Institute of Standards and Technology and is a free software released under the terms of the General Public License (<http://www.isd.mel.nist.gov/projects/rcslib/>, <http://www.linuxcnc.org/>).

The development of the machining robot control system prototype comprised a number of stages. For testing the functions of inverse and direct kinematics, robot offline programming, control system behavior testing in real-time and collision detection, a virtual robot is configured.

4.1 Structure of the control system

Figure 8 shows a simplified structure of the first prototype of low-cost control system where EMC2 software as a basic component is indicated.

EMC2 software system (<http://www.linuxcnc.org/>) is composed of four modules:

- Motion controller (EMCMOT),
- Discrete I/O controller (EMCIO),
- Task coordinating module (EMCTASK), and
- Graphical user interface (GUI).

Of these four modules, only EMCMOT is a real-time module. The communications between a real-time module EMCMOT and non-real-time module EMCTASK are implemented either by shared memory or RT-Linux FIFO mechanisms.

EMCMOT module performs trajectory planning, direct and inverse kinematics calculations, and computation of desired outputs to motor drivers. All I/O functions, which are not directly related to the actual motions of machine axes, are handled within EMCIO module.

EMCTASK module is a task level command handler and program interpreter for the RS-274 NGC machine tool programming language, commonly referred to as a G-code.

Several user interfaces have been developed for EMC2 software system. AXIS is the most advanced GUI, featuring interactive G-code previewer. It is expanded to specific application needs of the proposed robotic machining system.

Hardware abstraction layer provides transferring of real-time data from EMC2 to robot control hardware or to virtual robot. During control system startup, a choice is made for a corresponding configuration between real or virtual robot control (Fig. 8). It is common to start up first the control system configuration for a virtual robot to visually detect possible collisions and to make final verification of the program. Connections to drivers from PC side are done via appropriate machine control interfaces including ADC, DAC, and I/O channels.

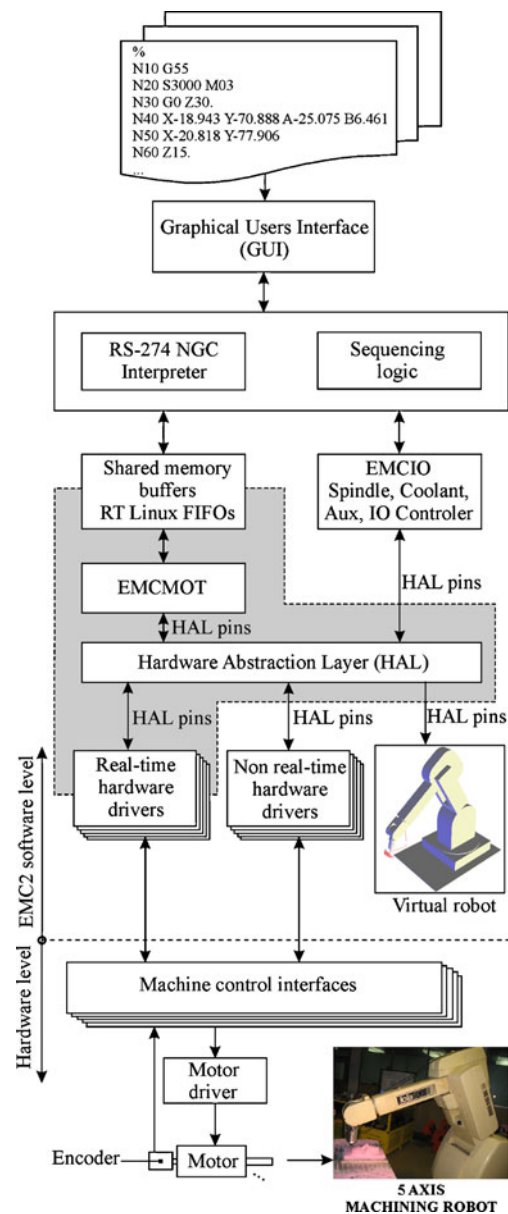


Fig. 8 Structure of the control system

4.2 Virtual robot

The virtual robot is configured using several predefined Python classes in EMC2. Based on inverse kinematics Eqs. 17, 19, 20, 27, 30 and direct kinematics Eqs. 15, 9, and 10, kinematic module is programmed in C language and is integrated in EMC2 software system (Fig. 8).

Figure 9 shows a detailed structure of the programming system and control system configuration for virtual robot control.

As obvious from Fig. 9, the part programming is very conventional with the use of a postprocessor to convert CL file into G-code. This means that the programmer starts

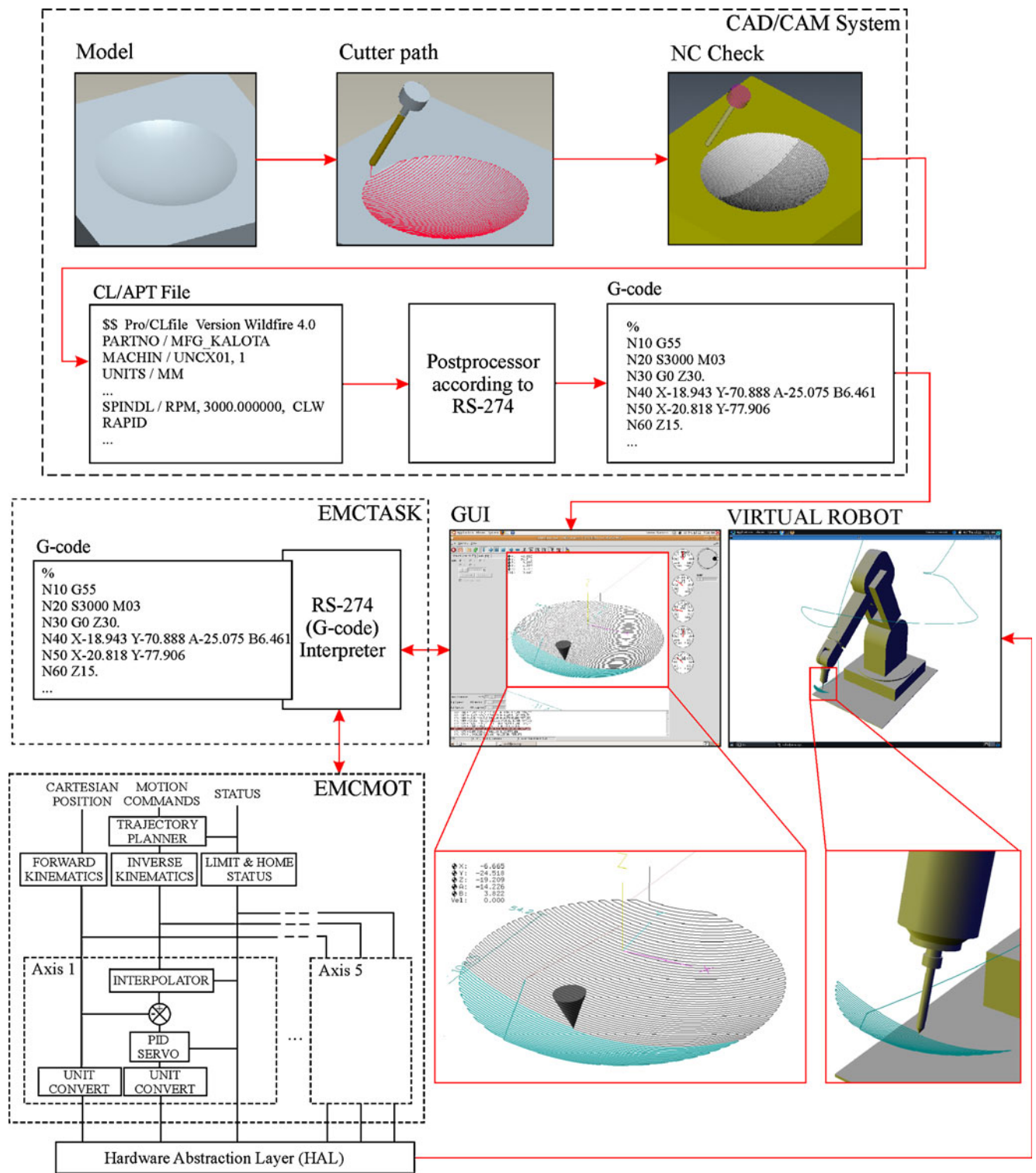


Fig. 9 Virtual robot control and programming

from the work piece CAD model in a common way, in this case in CAD/CAM system Pro/Engineer, generating CL file. The generated tool path is tested through the NC check (animated display of tool path and material removal). Using

the configured postprocessor for the vertical five-axis milling machines (X, Y, Z, A, B) spindle-tilting type, post-processing of CL file is done to obtain the robot program in G-code, which is transferred to the robot control system.

In this stage of development, the system makes possible to work with parallel coordinate frames $\{M\}$ and $\{W\}$ only (Fig. 3). In this case, the tool tip position vector and unit vector of tool axis z_T in robot reference frame $\{M\}$, according to Eqs. 2 and 3, become

$${}^M \mathbf{p}_T = [x_M \ y_M \ z_M]^T = {}^M \mathbf{p}_{O_w} + {}^W \mathbf{p}_T \quad (34)$$

$${}^M \mathbf{k}_T = {}^W \mathbf{k}_T = [k_{Tx} \ k_{Ty} \ k_{Tz}]^T \quad (35)$$

where ${}^M \mathbf{p}_{O_w} = [x_{O_w} \ y_{O_w} \ z_{O_w}]^T$ is the position vector of the origin of work piece frame $\{W\}$.

If the robot is initialized and tool and work piece setting is done, the program can be tested in two ways (Fig. 9). First, during G-code loading, EMC2 software displays the programmed tool path. However, the second way is of crucial importance, because it employs a virtual robot. The virtual robot enables final verification of G-code that includes the following:

- Check if the robot can execute the specified paths within the limited joints motions ranges and speeds
- Visual detection of collisions between the robot and tool with work piece and jigs and fixtures

After these verifications, the program can be safely executed on the real robot.

5 Experiments

Experiments were conducted to machine three test work pieces of light materials using experimental robot from Fig. 2. The setting of robot reference position and elementary calibration was performed by robot manufacturer’s experts as their contribution to this research. The main goal of the experiments was to test capabilities of the developed control system prototype. The CAD/CAM system Pro/Engineer was used for the experiments with the idea that the programming of machining robot and machining itself is done in exactly the same way as it is done on a five-axis vertical milling machine (X, Y, Z, A, B) spindle-tilting type.

Prior to machining, the programs are tested in two ways:

- by graphical simulation of tool paths in EMC2
- on virtual robotic machining system to perform the final verification of the program and to visually detect possible collisions, because virtual machining system, apart from virtual robot, involves virtual work piece and jigs and fixtures

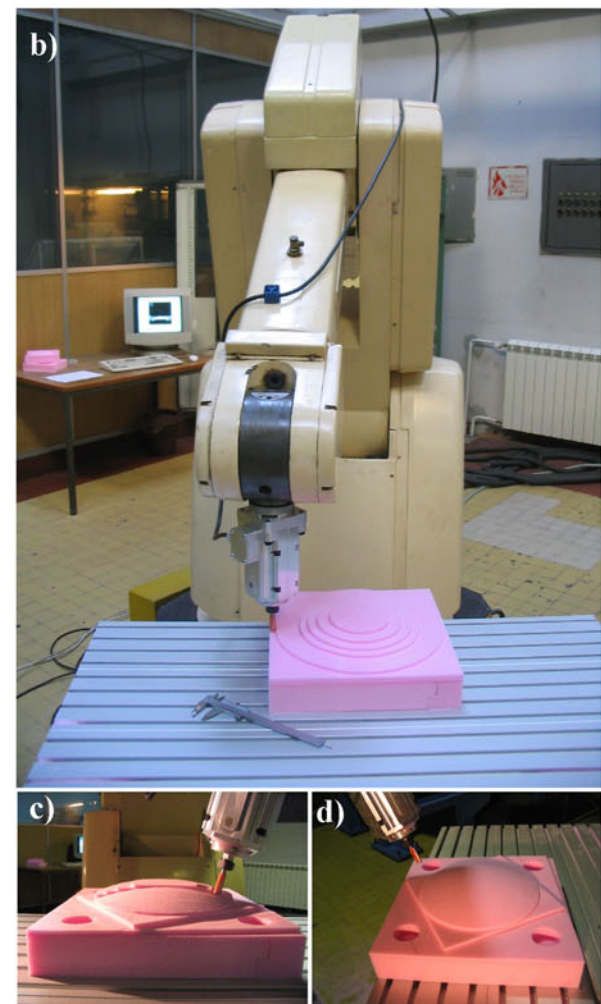
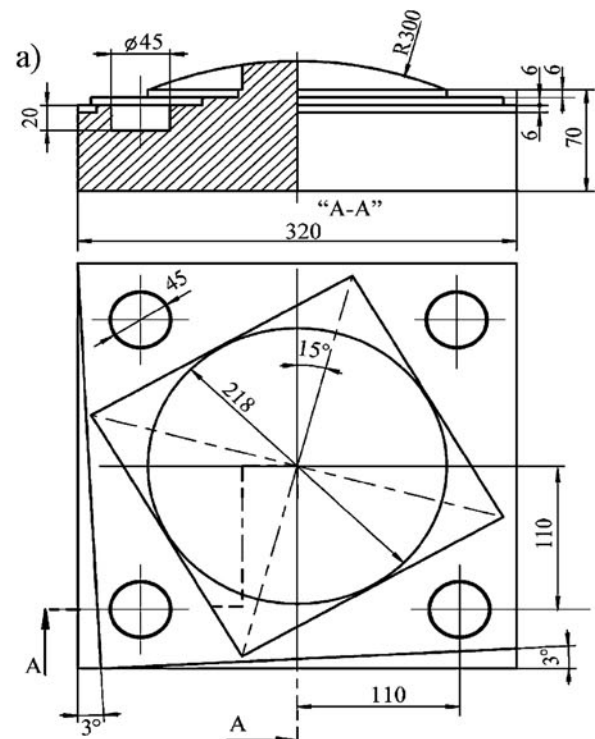


Fig. 10 a–d First test work piece machining

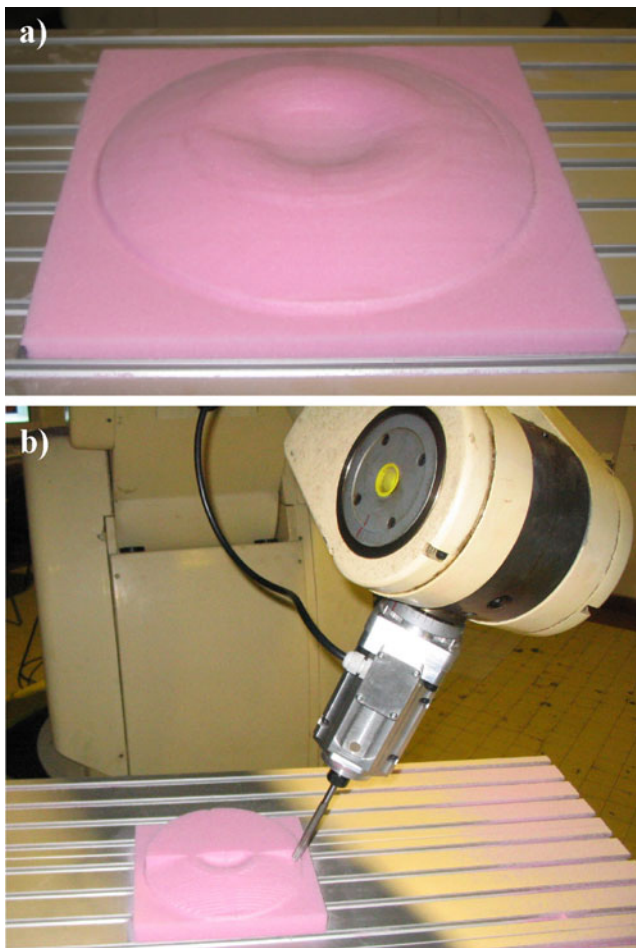


Fig. 11 a, b Second test work piece machining

The experiments were organized to embrace three- and five-axis machining of analytical and freeform (or sculptured) surfaces. For these three test work pieces (Figs. 10, 11, and 12), Styrofoam was used, which is especially suited to this kind of experiment as the process forces are rather low, minimizing the possibility of damage due to unexpected vibrations.

The first test work piece (Fig. 10a) was designed similar to the test pieces suggested by various standards to enable a simple test of robot programming ability to produce standard features. Figure 10b shows three-axis machining which also involves pre-machining for five-axis machining of calotte (Fig. 10c). In both cases, a flat endmill (tool/flute length 60/30 mm, diameter 12 mm) was used. The finished test work piece is presented in Fig. 10d.

Figure 11a shows the second test work piece with complex analytical surface consisting of two spherical surfaces whose connection is rounded, with a toroidal surface. Figure 11b displays five-axis finishing which is executed after three-axis pre-machining. In both cases, a ball-endmill (tool/flute length 140/80 mm, diameter 11 mm)

was used. This example was interesting because of intensive changes in tool orientation in a wide range, when machining the rounded surface between concave and convex spherical surfaces.

Figure 12 shows three- and five-axis machining of freeform surfaces on the third test work piece having the shape of human face. Figure 12a presents the pre-machined work piece during the three-axis roughing, while Fig. 12b presents five-axis finishing in the final stage. For this test work piece, the tool used in the previous example was employed.

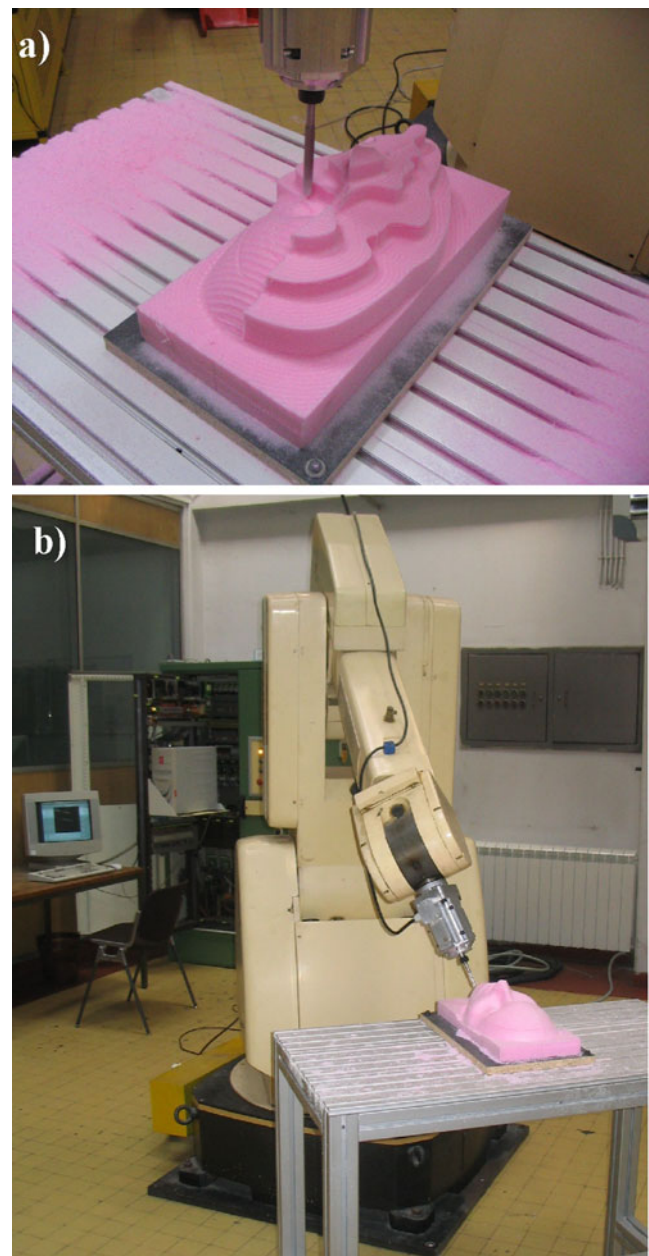


Fig. 12 a, b Third test work piece machining

These experiments confirmed that it is possible to realize the low-cost robotic machining system for the complex-surface parts of light materials and lower tolerance, which can be directly used by CNC machine tools programmers and operators.

6 Conclusion

The paper presents the concept of reconfigurable robot based multi-axis machining system for machining in one place complex parts of light materials with lower tolerances having freeform surfaces. The proposed concept is based on five-axis vertical articulated robot considered as a specific configuration of five-axis vertical milling machine (X, Y, Z, A, B) spindle tilting type and possibilities of programming in G-code. For basic configuration of the five-axis robotic machining system, robot modeling approach is shown in detail as well as the prototype of the developed low-cost control and programming system based on EMC2 software system. Verification of the experimental robotic machining system is presented using the examples of machining of three test work pieces of light materials. The shown examples of test work pieces comprised three- and five-axis machining of analytical and freeform surfaces, where programming and the machining itself were performed according to the procedure applied for CNC machine tools. The developed and investigated experimental robotic machining system indicates that such commercial system may be superior to the compatible robotic machining solutions, considering the G-code is still very widely used in industry. The subsequent stages of research will involve the development of specialized five-axis vertical articulated machining robot and control system that will enable three- and five-axis machining by various combinations of robot's axes and additional rotational and translational axes.

Acknowledgement The authors would like to thank the Ministry of Science and Technological Development of Serbia for providing financial support that made this work possible.

References

- Abele E, Kulok M, Weigold M (2005) Analysis of a machining industrial robot. Proc 10th International Scientific Conference on Production Engineering-CIM2005, Lumbarda, Croatia, pp II 1–11
- Pan Z, Zhang H (2008) Robotics machining from programming to process control: a complete solution by force control. *Ind Robot Int J* 35(5):400–409. doi:10.1108/01439910810893572
- Vergeest JSM, Tangelder JWH (1996) Robot machines rapid prototype. *Ind Robot* 23(5):17–20. doi:10.1108/01439919610130328
- Shirase K, Tanabe N, Hirao M, Yasui T (1996) Articulated robot application in end milling of sculptured surface. *JSME Int J Ser C* 39(2):308–316
- Chen YH, Hu YN (1999) Implementation of a robot system for sculptured surface cutting. Part 1. Rough machining. *Int J Adv Manuf Technol* 15:624–629. doi:10.1007/s001700050111
- Hu YN, Chen YH (1999) Implementation of a robot system for sculptured surface cutting. Part 2. Finish machining. *Int J Adv Manuf Technol* 15:630–639. doi:10.1007/s001700050112
- Song Y, Chen YH (1999) Feature-based robot machining for rapid prototyping. *Proc Instn Mech Engrs B* 213(5):451–459. doi:10.1243/0954405991516921
- Gerke W (2004) Milling robot with 3D vision system for styrofoam modelling. Proc IEEE International Conference on Mechatronics and Robotics part II, Aachen, pp 192–196
- Abele E, Weigold M, Rothenbuecher S (2007) Modeling and identification of an industrial robot for machining applications. *Annals of the CIRP* 56(1):387–390. doi:10.1016/j.cirp.2007.05.090
- Shin-ichi M, Kazunori S, Nobuyuki Y, Yoshinari O (1999) High-speed end milling of an articulated robot and its characteristics. *J Mater Process Technol* 95:83–89. doi:10.1016/S0924-0136(99)00315-5
- Olabi A, Bearee R, Gibaru O, Damak M (2010) Feedrate planning for machining with industrial six-axis robots. *Control Engineering Practice* 18(5):472–482. doi:10.1016/j.conengprac.2010.01.004
- Li W, Red E, Jensen G, Evans M (2007) Reconfigurable mechanisms for application control (RMAC): applications. *Comp Aided Des Appl* 4(1–4):549–556. ISSN 1686-4360
- DePree J, Gesswein C (2008) Robotic machining white paper project-Halcyon Development, <http://www.halcyondevelop.com>
- Milutinovic D, Glavonjic M, Zivanovic S, Dimic Z, Slavkovic N (2009) Development of robot based reconfigurable machining system. Proc 33rd Conference on Production Engineering of Serbia, Belgrade, pp 151-155 ISBN 978-86-7083-662-4
- Lee RS, She CH (1997) Developing a postprocessor for three types of five-axis machine tools. *Int J Adv Manuf Technol* 13(9):658–665. doi:10.1007/BF01350824
- Affouard A, Duc E, Lartigue C, Langeron JM, Bourdet P (2004) Avoiding five-axis singularities using tool path deformation. *Int J Mach Tools Manuf* 44:415–425. doi:10.1016/j.ijmactools.2003.10.008
- Shin SJ, Suh SH, Stroud I (2007) Reincarnation of G-code based part programs into STEP-NC for turning applications. *Comput-Aided Des* 39:1–16. doi:10.1016/j.cad.2006.08.005
- ISO 841:2001 Industrial automation systems and integration—Numerical control of machines—Coordinate system and motion nomenclature
- Paul RP (1981) Robot Manipulators: mathematics, programming and control. MIT, Boston
- Fu KS, Gonzalez RC, Lee CSG (1987) Robotics: control, sensing, vision, and intelligence. McGraw-Hill, New York
- Craig JJ (1989) Introduction to robotics: mechanics and control, 2nd edn. Addison-Wesley, New York
- Spong MW, Vidyasagar M (1989) Robot Dynamics and Control. Wiley, Chichester
- Manseur R, Doty KL (1992) Fast inverse kinematics of five-revolute-axis robot manipulators. *Mech Mach Theory* 27(5):587–597. doi:10.1016/0094-114X(92)90047-L
- Pashkevich A (1997) Real-time inverse kinematics for robots with offset and reduced wrist. *Contr Eng Pract* 5(10):1443–1450. doi:10.1016/S0967-0661(97)00142-1
- Innocenti C, Parenti CV (1994) Exhaustive enumeration of fully parallel kinematic chains. *Dyn Syst Contr* 55:1135–1141
- Glavonjic M, Milutinovic D, Zivanovic S, Dimic Z, Kvrivic V (2010) Desktop three-axis parallel kinematic milling machine. *Int J Adv Manuf Technol* 46(1–4):51–60. doi:10.1007/s00170-009-2070-3